Clinical Neurophysiology 130 (2019) 2169–2181

Contents lists available at ScienceDirect

Clinical Neurophysiology

journal homepage: www.elsevier.com/locate/clinph

Cognitive effort decreases beta, alpha, and theta coherence and ends afterdischarges in human brain

Ronald P. Lesser [a,b,*], W.R.S. Webber [a], Diana L. Miglioretti [c,d], Jay J. Pillai [e], Shruti Agarwal [e], Susumu Mori [e], Peter F. Morrison [a,1], Stefano Castagnola [a,2], Adeshola Lawal [a,4], Helen J. Lesser [a,3]

[a] Department of Neurology, Johns Hopkins University School of Medicine, Baltimore, MD 21287, USA
[b] Department of Neurosurgery, Johns Hopkins University School of Medicine, Baltimore, MD 21287, USA
[c] Department of Public Health Sciences, University of California, Davis, School of Medicine, Davis, CA 95616, USA
[d] Kaiser Permanente Washington Health Research Institute, Seattle, WA 98101, USA
[e] Department of Radiology and Radiological Science, Johns Hopkins University School of Medicine, Baltimore, MD 21287, USA

See Editorial, pages 2164–2165

ARTICLE INFO

Article history:
Accepted 12 July 2019
Available online 19 July 2019

Keywords:
Afterdischarges
Cognition
Attention
Effort
Coherence

HIGHLIGHTS

- Cognitive effort causes changes that are not limited to specific functional networks.
- Cognitive effort can end afterdischarges in regions not functionally related to the cognitive task.
- When afterdischarges end there are widespread coherence decreases within specific frequency ranges.

ABSTRACT

Objective: Mental activation has been reported to modify the occurrence of epileptiform activity. We studied its effect on afterdischarges.
Method: In 15 patients with implanted electrodes we presented cognitive tasks when afterdischarges occurred. We developed a wavelet cross-coherence function to analyze the electrocorticography before and after the tasks and compared findings when cognitive tasks did or did not result in afterdischarge termination. Six patients returned for functional MRI (fMRI) testing, using similar tasks.
Results: Cognitive tasks often could terminate afterdischarges when direct abortive stimulation could not. Wavelet cross-coherence analysis showed that, when afterdischarges stopped, there was decreased coherence throughout the brain in the 7.13–22.53 Hz frequency ranges (p values 0.008–0.034). This occurred a) regardless of whether an area activated on fMRI and b) regardless of whether there were afterdischarges in the area.
Conclusions: It is known that cognitive tasks can alter localized or network synchronization. Our results show that they can change activity throughout the brain. These changes in turn can terminate localized epileptiform activity.
Significance: Cognitive tasks result in diffuse brain changes that can modify focal brain activity. Combined with a seizure detection device, cognitive activation might provide a non-invasive method of terminating or modifying seizures.

Abbreviations: AD, afterdischarge; ADs, afterdischarges; AST, arithmetic or spelling task; BPS, brief pulse stimulation; ECoG, electrocorticography; EDF, European Data Format; fMRI, functional magnetic resonance imaging; WxCoh, wavelet cross-coherence; μC, microcoulombs.

* Corresponding author at: Department of Neurology, Johns Hopkins University School of Medicine, Baltimore, MD 21287, USA.
E-mail address: rl@jhmi.edu (R.P. Lesser).
[1] Current address: Tufts University School of Medicine, Maine Medical Partners Neurology, Scarborough, ME 04074, USA.
[2] Current address: Sidney Kimmel Medical College, Thomas Jefferson University, Philadelphia, PA 19107, USA.
[3] Current address: Philadelphia College of Osteopathic Medicine, Philadelphia, PA 19131, USA.
[4] Current address: Whiting School of Engineering, Johns Hopkins University, Baltimore, MD 21218 USA.

https://doi.org/10.1016/j.clinph.2019.07.007
1388-2457/

1. Introduction

Epilepsy is one of the most common and burdensome neurological disorders. Although medications usually control seizures, seizures continue in up to 30% of patients (Gooneratne et al., 2016). The medical intractability of seizures has led to the development of implantable devices using electrical stimulation to treat seizures. With currently available devices, seizures decreased by half in about two-thirds of patients, but complete seizure control is rare (Gooneratne et al., 2016). Thus, there is need for new approaches for treating seizures.

A routine part of the surgical care of many patients with intractable epilepsy is electrical brain stimulation to localize regions important for motor, sensory, or language processes. An unwanted side effect of this stimulation is the occurrence of afterdischarges **(ADs),** epileptiform brain discharges which can evolve into clinical seizures. We have previously shown that brief pulse stimulation **(BPS)** at the sites producing ADs can terminate them but is only successful about half the time (Lesser et al., 1999). Penfield and Jasper showed an example of an arithmetic task temporarily arresting epileptiform activity (Penfield and Jasper, 1954). We have found that arithmetic or spelling tasks **(AST)** at times can terminate ADs permanently when direct stimulation cannot.

In a recent report (Muldoon et al., 2018) we (RPL, WRSW) and others showed that local brain states during ASTs affected the likelihood that ADs would stop in response to ASTs. The ability to locate regions that underlie the occurrence of clinical phenomena has importantly advanced our understanding of how the brain works. However, we show here that the electrophysiologic correlates to AD suppression are not limited to regions where ADs are located, or which modulate AST tasks used to suppress the ADs: there are changes throughout the cortex. This suggests that activity involving the whole brain at times may be as important as regional changes.

2. Materials and methods

2.1. Patients

We reviewed the recordings of all patients who had intracranial electrodes placed for evaluation of intractable seizures and had undergone clinical stimulation testing over a 4-year period. In 15 of these patients, a cognitive intervention was used in an attempt to abort ADs. (Arithmetic or spelling tasks were used; see below.) A different aspect of our findings in these patients has previously been reported (Muldoon et al., 2018). There were 7 males and 8 females, age 12–53 years. None of these patients reported seizures precipitated by calculation, spelling, or similar mental activities. Clinical considerations alone determined electrode locations, number of electrodes placed, duration of recording, number and duration of testing sessions, electrodes stimulated, and modalities (see below) tested. Anticonvulsant medications varied among these patients, again based on clinical considerations alone. However, we report changes occurring over the span of a few seconds, and there were no within patient medication changes over those brief periods of time. Supplemental Table 1 gives additional patient information. The data review for this report was approved by our Institutional Review Board, as were the informed consent and testing protocols used for the functional magnetic resonance **(fMRI)** studies performed on six patients that returned and on 9 controls. The two patients whose testing is excerpted in the Supplemental Movies gave consent for the use of these for this report.

2.2. Recordings

We recorded from a total of 1276 electrodes. The electrodes were 4 mm diameter (2.3 mm exposed to the cortex, 10 mm center to center distance) 1.5 mm thick subdural discs or 1.1. mm diameter, 5- or 10-mm spacing depth electrodes, made of platinum (Ad-Tech Medical Instrument Corporation, Racine, Wisconsin, USA), embedded in flexible silastic in linear or rectangular arrays and placed in the subdural space or implanted into the cortex. Cylindrical depth electrodes were used at times. These were 1.1 mm diameter, 1.32- or 2.41-mm length, spaced 2.2 mm or 6.5 mm apart (Ad-Tech Medical Instrument Corporation, Racine, Wisconsin, USA.) Electrode location with respect to underlying cortical gyral anatomy was determined by direct observation in the operating room and by co-registration of pre-implantation volumetric brain MRI (1–1.8 mm coronal slice thickness) with post-implantation volumetric brain CT (1 mm axial slice thickness) in all patients according to anatomic fiducials using Curry (Compumedics Neuroscan, El Paso, TX, USA). Electrode positions derived from post-implantation CT scans were displayed with a brain surface rendering derived from the pre-implantation MRI. (Supplemental Figs. S4–S21.)

Patients underwent continuous electrocorticography (ECoG) using a Stellate Harmonie (Natus Medical Incorporated, Pleasanton, CA 94566 USA) system that was capable of recording up to 128 channels with 1000 samples per second per channel, using Schwarzer EEG Amplifiers Model 210033 (Natus Europe GmbH, Robert-Koch-Str. 1, Planegg, Germany). Video sampling rate was 30 frames per second. The machines used 16-bit A-D converters (Gain 1408, Range 4.5 Volts, Noise referred to input 1.5 Microvolts). The low-pass anti alias filter was set to 300 Hz (20 dB/Oct Butterworth 5th Order) and high-pass to 0.0016 Hz (6 dB/Oct RC 1st Order). Analog to digital conversion was 16 bits with Least Significant Bit (LSB) equal to 0.10 Microvolts, peak to peak noise 1.5 Microvolts (equivalent to 4 bits), and Common Mode Rejection Ratio (CMMR) of 100 dB. A common average reference was used for the recordings. Since we did not know in advance where ADs might occur, we could not modify the reference for specific trials. The analyses themselves were done between electrode pairs, and not between individual electrodes and the reference. In all cases recordings were continuous from all implanted electrodes. The complete localizing stimulation testing sessions, each lasting about two hours, were exported in European Data Format **(EDF)** (Kemp et al., 1992) for analysis at a later date.

2.3. Clinical testing

Extraoperative functional mapping was performed using electrical stimulation via the implanted electrodes, gradually increasing stimulus intensity as previously described to as high as 15 milliamperes (mA), the maximal possible with our device, a Grass S12 stimulator (Astro-Med, Inc., West Warwick, RI. 02893 USA) (Lesser et al., 1984; Lesser et al., 1994). Charge for each pulse train was measured using a custom-built circuit and was recorded along with the ECoG. Stimulation used pairs of opposite polarity charge balanced square wave pulses, 0.3 ms in duration, repeated at 50 pulses per second. Maximal stimulation current actually used in these patients was 12 mA, with a charge of 3.6 microcoulombs (μC) per pulse. Pulse trains for the stimulation testing were 2–5 s long. For a 2 s period of stimulation there were 100 pulses, and, at 12 mA, a total of 360 μC were delivered. There were 5 pulses in each train of BPS. With the exception of total train duration, BPS parameters were otherwise identical to those just used for the stimulation testing. As just noted, there were 3.6 μC per pulse or a total of 18 μC for each BPS train of 5 pulses, when stimulating at 12 mA. As would be expected, since charge is linear, charge was 9 μC at 6 mA, 6 μC at 4 mA, etc. When BPS successfully ended ADs, charge was 9.9 ± 4.8 μC. When BPS did not end ADs, charge was 9.5 ± 5.5 μC. Stimulation usually was between electrodes that were adjacent to one another; the figures show exceptions. Note that the current density produced by stimulation is maximal in the region

of the electrodes tested, drops off rapidly, and is much lower in between electrodes, even for adjacent electrodes (Lesser et al., 1994).

Patient testing occurred in their hospital rooms, with patients lying supine, with the head of the bed elevated. Patients would initially lie quietly, while stimulus intensity was slowly increased. During this they would indicate whether they noticed any motor or sensory changes occurring in response to stimulation, and testing personnel would look for motor changes. Specific tests and locations tested varied according to the patient, based on clinical need, but, overall, once stimulus intensity had been optimized for a given site without sensorimotor changes occurring, patients next would be tested for inhibition of activity while performing rapid alternating movements of eyes, tongue, fingers or toes, while naming objects taken from the Boston naming test, while speaking, reading or repeating single words, or reading passages of text, while following commands, or during auditory responsive naming (i.e. where do you put food in the kitchen to keep it cold?) (Lesser et al., 1986; Hamberger et al., 2001). In three patients (S2, 8, 14) neglect was tested (line bisection, gap detection, shape judgment, reading left/right visual field), with findings in S8 and S14. Two patients, whose occipital lobes were tested, also reported flashing lights with stimulation. See Supplemental Figs. S4–21 for additional information regarding the stimulation results. There were 47 testing sessions, lasting an average of 71 minutes; the longest was 216 minutes. We emphasize again that the choice of sites to test, and the modalities to test, were based on clinical needs alone. Also, stimulation at times can evoke pain at a particular electrode (Lesser et al., 1985), so that testing cannot be performed at that site. For all these reasons, not all electrodes and modalities were tested.

During testing, ongoing ECoG was monitored continuously for ADs (Lesser et al., 1999; Blume et al., 2004; Pouratian et al., 2004). ADs occur as abrupt changes in the ongoing ECoG, occurring after brain stimulation, but they vary in morphology (Penfield and Jasper, 1954; Lesser et al., 1999; Blume et al., 2004; Liu et al., 2017) and thresholds for evoking ADs vary from site to site and trial to trial, even when testing and retesting over short intervals(Lesser et al., 1984; Pouratian et al., 2004; Lesser et al., 2008). In these patients, we found ADs of four types (1) continuous sinusoidal, (2) continuous quasi-sinusoidal appearance but spike-like morphology or sharp point at extreme of discharge, (3) repeated bursts with pause of epileptiform activity in between, (4) spike-and-slow-wave complex. Stimulation did not induce the habitual seizures for these patients (Kovac et al., 2014).

When ADs occurred, the testing team observed the ECoG to see if ADs stopped spontaneously. Electrical stimulation can transiently saturate the EEG amplifiers after stimulation, possibly obscuring any ADs that might be present, a phenomenon called blocking. Because of this, testing personnel waited at least two seconds to ascertain whether an ADs continued (Lesser et al., 1999). If ADs did not stop, an effort was made to terminate them: brief pulses of electrical stimulation were given at the same electrode pair where stimulation had produced the ADs (Lesser et al., 1999), or the patient might be asked to solve arithmetic problems (i.e. what is 27 + 14, what is 73 – 6, or (patient S1) count backwards) (Penfield and Jasper, 1954), or asked to spell words backwards, or (patient S1) to recite the alphabet backwards. ADs vary considerably with respect to when they occur and how long they last. Because of this, once ADs were noted, the length of time to wait before using BPS or AST was a clinical decision on the part of the testing team. There were no specific instructions regarding whether or not to use BPS or AST, or regarding what task to present to the patient when AST was used.

The patients were likely aware that ADs were occurring because of the reactions of the testing personnel but were given the cognitive tasks without any other specific warning. Patients recognized all the numbers and words they were asked. Tasks were used during testing in either hemisphere, were used whether or not ADs were in a region which literature has suggested might be important for arithmetic or spelling, and were used whether or not the AST had been preceded by BPS (Morris et al., 1984; Lesser et al., 1986; Whalen et al., 1997; Duffau et al., 2002; Bitan et al., 2005; Philipose et al., 2007; Dastjerdi et al., 2013).

Electrodes stimulated, intensities used, changes produced by stimulation, occurrence of ADs, and effects of interventions (brief pulses of stimulation, arithmetic, spelling) were recorded in real time using locally developed (RPL) program, called Report.

2.4. Functional MRI

Six of the 15 patients returned for post-resection functional MRI studies (S1,2,6,7,9,13), 3 males and 3 females (all 15 were invited). When they came for functional MRI, they were ages 19–57). We compared their findings to those of 9 control subjects, 3 male and 6 females, ages 22–62). All 15 were of normal intelligence and were right-handed. Commercially available structural sequences were used for anatomical imaging including a T1 weighted 3D MPRAGE sequence for primary anatomic overlay of functional activation maps. BOLD functional MRI acquisitions involved a standard single shot gradient echo EPI pulse sequence. Our Institutional Review Board approved the study.

The goal was to use fMRI paradigms that were as similar as possible to the tasks used during stimulation testing to best reflect the cortical regions that might have been active during stimulation testing. All of the tasks (paradigms) described below were performed by the subjects while inside the bore of a 3.0 Tesla MRI scanner during continuous image acquisition utilizing single shot gradient echo EPI pulse sequences for blood oxygen level dependent (BOLD) magnetic resonance imaging (functional MRI). Prior to patient placement into the MRI scanner, a detailed pre-scan training session was conducted outside the MRI scanner to familiarize the subjects with the tasks to be performed and to assess their ability to adequately perform these tasks. Additional task-specific instructions were given to the subjects while they were inside the scanner prior to running each paradigm.

All problems were presented through earphones, with choices on a rear projection screen.

For each paradigm, there was a simple task, a more complex task, and a control task. Auditory stimulus presentation was used. The total time for each paradigm was 7 minutes. The subject performed each task covertly, i.e., silently in the subject's mind without any overt vocalization, since such vocalization could induce undesirable bulk head motion that could invalidate the fMRI results. Button press was used at the end to indicate the correct answer.

Each paradigm consisted of 3 repetitive cycles. Each cycle was 135 s in duration and consisted of three blocks of 45 s each. In each 45 s block, the first 5 s were dedicated to introduction of the block and next 40 s were for the actual performance of the tasks, with each task presented for 5 s. Hence each cycle had alternating 45 s blocks of simple, more complex, and control tasks.

2.4.1. Paradigm 1: Mental arithmetic computation

For the arithmetic part of the fMRI study, the subject was asked to subtract a 1-digit number from a 2-digit number. For the "simple" task, the first digit of the two-digit number did not change after subtraction (for example 84 – 2 = 82). For the more difficult task it did (for example 84 – 7 = 77). The subject heard the problem and was shown two choices on the screen and had to select whether the left or right choice was correct.

For the control task the subject was asked to listen to a subtraction problem (for example 87 − 3) and to indicate whether the first of the two numbers (i.e. 87) was even or odd.

2.4.2. Paradigm 2: Spelling

For the spelling part of the study patients were presented with 3 ("simple" task) or 5 ("difficult" task) letter words and asked to choose from the screen the correct reverse spelling of the word (for example "storm" spelled backwards is M-R-O-T-S. An alternate choice might be M-R-T-O-S.

For the control task, the subjects heard a word and were asked to choose whether the first letter was a consonant or a vowel.

The words selected were one syllable words with no consecutive identical letters, no silent letters, no consecutive vowels, no plurals, no past tense. For five letter words the source was http://www.math.toronto.edu/jjchew/scrabble/lists/common-5.html. For three letter words the source was http://www.scrabble.org.au/words/threes.htm. Patients recognized all the words they were asked.

The side of button press for the correct answers were initially by coin flip, with final choices then counterbalanced so that half of the correct answers were on the left and half on the right.

2.5. Figure preparation, stimulation results

As part of their routine clinical care, electrode locations were visually noted and documented in the operating room. In addition, the location of electrodes relative to the cortical surface was determined by co-registering volumetric brain MRI (1–1.8 mm coronal slice thickness), obtained before surgery, with volumetric brain CT, obtained after the electrodes were in place. The MRI and CT images were co-registered using Curry (Compumedics, Charlotte, North Carolina 28269 USA) or BioImage (bioimagesuite.yale.edu) so as to indicate the location of the implanted electrodes relative to the underlying cortical surface anatomy (Sinai et al., 2005). The resulting reconstructions were imported into Photoshop (Adobe Systems, San Jose, California, USA), and annotations indicating the results of stimulation were superimposed on the reconstructions, also using Photoshop. Additional explanatory labeling and annotations for Fig. 3,4, and S1–S3, and for the Key for Figs. S1-S21 were prepared using PowerPoint 2016 (Microsoft Corporation, Redmond, Washington USA).

2.6. Analysis of electrocorticography

Among the 15 patients studied, there were 116 trials during which ADs occurred and during which an arithmetic or spelling task was used in an attempt to stop the ADs. The number of trials per subjects varied from 1 to 36, and the number of electrode pairs varied across subjects and trials from 1540 to 5886 (Supplemental Table 1). The numbers 1540 to 5886 reflect the actual number of pair combinations analyzed. This included all possible combinations of 2 electrodes among the monitored electrodes, where the order of the 2 electrodes did not matter, i.e. combinations not permutations. For example, for 4 electrodes, called A, B, C, and D, the possible combinations are AB, AC, AD, BC, BD, CD. The absolute polarity of the waveform recorded from A to B would differ from the waveform recorded from B to A. However, results of coherence calculations, such as we performed, would be the same.

We analyzed two 4000 msec periods, the first occurred before an arithmetic or spelling task had been given. We call this E1 – indicating the first analyzed four second epoch. The second began after the tester had begun to state the arithmetic or spelling problem. We call this E2 – indicating the second analyzed four second epoch. (See Fig. 3 and Supplemental Figs. S1–S3.)

Analysis of the records was done using two programs, VZ7.exe and WCC5.exe, both locally developed (WRSW) programs written in 'C'. To view ECoG we used VZ7.exe, which allowed us to review and measure both the ECoG and video at any desired level of accuracy, down to the millisecond. VZ7.exe contains calculation modes within it, and allows export to MATLAB (MathWorks, Natick, MA 01760 USA). VZ7.exe allowed marking EDF files with the times of the E1 and arithmetic or spelling task sections to be analyzed. The times of the cognitive task questions and answers were also marked with VZ7.exe so that positions of the all the relevant events in each trial could be seen at the same time on one screen. To assess the degree of synchrony in the ECoG, we calculated mean wavelet cross-coherence (see below) between all pairs of implanted electrodes using WCC5.exe. WCC5.exe uses the events marked with VZ7.exe to locate the sections of the ECoG where wavelet cross-coherence measurements are made.

Brain rhythms traditionally are divided into several groups, for example, delta (below 4 Hz), theta (4–7 Hz), alpha (8–13 Hz), beta 14–40 Hz), and gamma (above 40 Hz) (Noachtar et al., 1999). There are differences between authors regarding the precise divisions between frequencies (see for example the Wikipedia entries for these). Although we use these terms in the general sense in this report, we used wavelet scales for our actual calculations.

We calculated wavelet cross-coherence for all electrode pairs over a range of wavelet scales from 300 to 1.69 Hz. For these calculations, a scale can be thought of as a surrogate for frequency. As indicated above, the data were analyzed for two 4000 msec windows containing ADs. The first, called E1, occurred before the arithmetic or spelling task and the second, E2, began after the tester had begun to state the arithmetic or spelling problem. The lengths of time for the questions to be asked and answered were such that ADs were present in all data segments analyzed, and no brief pulses of stimulation were present. Longer sections would have overlapped brief pulses of stimulation events in some cases.

2.6.1. Wavelet cross-coherence

The hypothesis is that when a cognitive task stops an AD it does so by disrupting the activity that sustains the AD. We are testing whether the changes can be reflected by a change in coherence of the electrical activity at some frequency. We measured coherence in all combinations of pairs of the recorded electrodes.

Initially we used a wavelet cross correlation function (Mizuno-Matsumoto et al., 2002) but found, as have others (Shaw, 1984), that in some cases the calculation failed to produce a peak in the correlation function, and a peak is needed to determine a cross correlation value. This is the risk in using cross correlation on short data sequences (Shaw, 1984).

Coherence is a similar measure of the relationship between signals that is the frequency domain equivalent of correlation in the time domain and has been used by several investigators to study seizure location and spread in intracranial recordings (Towle et al., 1999; Kramer et al., 2011; Martinet et al., 2017). The wavelet cross-coherence function devised here always produces a result because cross-coherence functions do not need to produce a peak. Studies have found wavelet coherence to be equivalent (Bruns, 2004) or superior (Klein et al., 2006) to Fourier base methods of measuring coherence. In addition, wavelet coherence can be used to study single trial brain signals. (Lachaux et al., 2002) The addition of wavelets localizes the measurements in both time and frequency (Najmi, 2012).

Encouraged by these previous results, we devised a simple method to calculate wavelet cross-coherence. This wavelet cross-coherence measure uses a wavelet formed by taking a fixed number of cycles of a sine and cosine wave to form a complex wave and then applying a Gaussian like exponential envelope to it. This then is a variant of the Morlet wavelet. The scale of this wavelet is

then dilated while keeping the number of cycles the same to form a lower frequency version. This process is repeated several times to produce a family of discreet wavelet scales that cover the whole frequency range for this data set. The step from one wavelet scale to the next is chosen with some overlap in frequency so that the whole frequency range is fully covered. The step from one wavelet to the next, in decreasing frequency, is given by:

$$F_{n+1} = F_n(C_y - C_s)/C_y \quad (1)$$

where:

F_n, F_{n+1} are the current and next wavelet frequency scales. The interval from one wavelet frequency to the next is a constant ratio, as explained in the next few sentences.

C_y is the number of cycles in the wavelet family. In this study it is set to 6.

C_s sets the spacing of the wavelets in scale, which sets the duration of the wavelet, and the difference in frequencies covered when moving from one scale to the next. Set to 1.5, this can be lowered to improve frequency coverage by making the wavelets closer in frequency.

With C_s = 1.5 and C_y = 6 the ratio of one wavelet frequency to the next is 0.75.

In this study, we have a total of 19 separate wavelets, each of which assess a different range of frequencies.

As C_s is increased the number of wavelets within the family of wavelets that would assess the total range of frequencies (from 1.69–300 Hz in this case) would be reduced after calculation of Eq. (1). The risk in doing this is that each of the separate wavelets could assess a narrower range of frequencies, so that some frequencies "between" two wavelets might not be appropriately assessed by either wavelet. (See next paragraph.)

The upper usable frequency limit of the data is 300 Hz set by the recording system anti-alias filter. The wavelet used consists of 6 cycles of a complex wave i.e. it has real (cosine) and imaginary (sine) parts (see Fig. 1). In this study we set $C_s = 1.5$in Eq. (2) below. This then covers the frequency range from 1.69 to 300 Hz in 19 wavelets in a logarithmic fashion such that the ratio of the frequency of adjacent wavelets is 1.33. That is, the next wavelet after the lowest frequency (1.69 Hz) wavelet is 2.26 Hz, the next after that is 3.01 Hz, and so on until the last and highest frequency wavelet is 300 Hz. The correlation between adjacent wavelets is 0.75, because there are no gaps in frequency space in the range of this study i.e. the coverage is continuous from 1.69 to 300 Hz. A family of wavelets with less overlap between adjacent wavelets would be less sensitive to frequencies in the regions shared by two adjacent wavelets. For example, in Fig. 2, if two adjacent wavelets are separated from each other to a greater extent on the X axis, the value on the Y axis in the regions of overlap would be lower, resulting in lower sensitivity to activity in those regions. To create a family of wavelets with virtually no overlap and gaps between them, i.e. with steep box like frequency response, we would need to use wavelets that would be several tens of seconds in duration and would be too long for this study. The lower frequency limit for this study is set by lowest frequency wavelet, 1.69 Hz that fits in the 4 s measurement period. For 6 cycles of 1.69 Hz the measurement period is 3.5 s. The next lower frequency wavelet in this sequence is 1.27 Hz and requires measurement period of 4.7 s, which would have been too long for the measurement period used in this study.

Although ADs do not appear visually to be simple sine waves, the basis of the wavelet used here is a sine wave. However, by changing C_y we can explore different wavelets. For example, larger values of C_y will produce wavelet families that are narrower in frequencies for which they are sensitive, but which will require a wider time window in order to differentiate a given frequency from a nearby frequency. The complex wavelet is then given by:

$$W_{un}(Fn,t) = e^{-kt^2}(\cos(2\pi F_n t) + j\,sin(2\pi F_n t)) \quad (2)$$

$$W(Fn,t) = \frac{W_{un}(Fn,t)}{\sqrt{\frac{\sum_{\tau=-W_{len}}^{\tau=+W_{len}} |W_{un}(F_n,\tau)|^2}{2}}} \quad (2.1)$$

where:

$$j = \sqrt{-1}$$

F_n is the frequency of the chosen wavelet derived from Eq. (1).

k is the taper for the Gaussian like exponential envelope and is chosen so that the amplitude of the wavelet at each end is 1.8% of the center amplitude. For $k = 1$ this is the Morlet wavelet.

t is the time index of the wavelet, with t = 0 in the middle of the wavelet. It runs from $-W_{len}$ to $+W_{len}$

$-W_{len}$, $+W_{len}$ are the limits of the wavelet e^{-kt^2} is the Gaussian-like envelope applied to the original waveform with k indicating the taper and t indicating the point along the wavelet

$W_{un}(Fn,t)$ is the un-normalized wavelet which is then normalized by dividing it by its root mean square (RMS) as shown in Eq. (2.1).

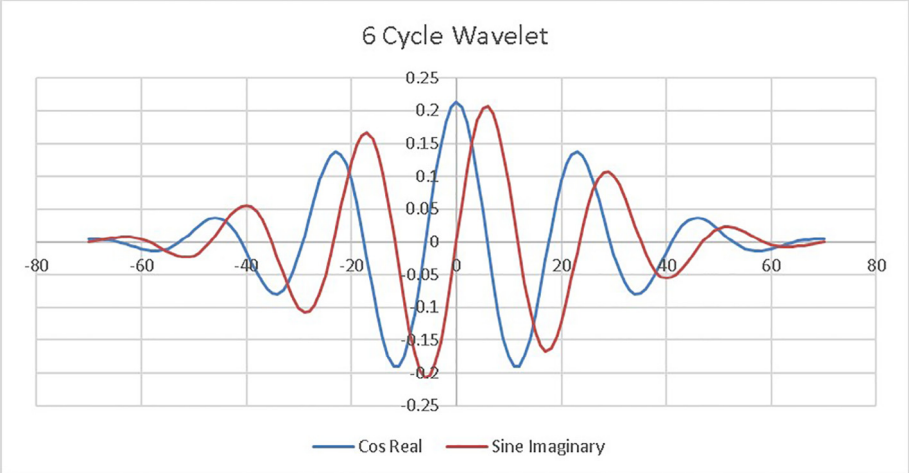

Fig. 1. Example Wavelet.

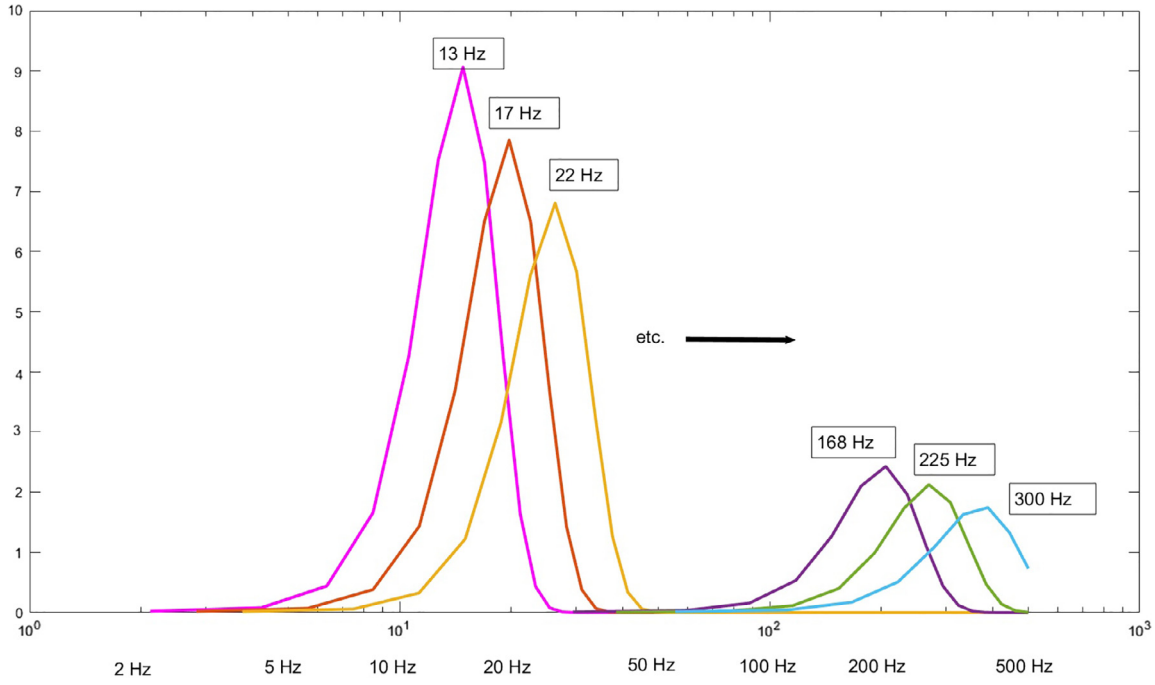

Fig. 2. Example of overlap between adjacent wavelets showing that the frequency space is covered continuously without gaps. The Y axis is in arbitrary units but reflects the sensitivity (i.e. frequency response) at the given point.

$W(F_{n,t})$ is the normalized wavelet used for the cross-coherence calculation.

For given wavelet *Fn* and a pair of electrodes *X* and *Y* we take a fixed length sample of data $X(t)$ and $Y(t)$. Each of these sample of data is convolved with the wavelet $W(Fn,t)$.

$$W_X(F_{n,}t) = \sum_{\tau=-W_{len}}^{\tau=+W_{len}} X(t-\tau)W(F_n,\tau) \tag{3}$$

$$W_Y(F_{n,}t) = \sum_{\tau=-W_{len}}^{\tau=+W_{len}} Y(t-\tau)W(F_n,\tau) \tag{3.1}$$

The wavelet cross-coherence value that we use is then given by the dot product of $W_X(F_n,t)$ and the conjugate of the same function for the other electrode, $*W_Y(F_n,t)$, and normalized by the amplitude of each sample of data $X(t)$ and $Y(t)$. The range of *WXCoh* is 0.0 to 1.0 due to normalization.

$$WXCoh_{X*Y}(F_n,t) = \frac{\sqrt{\sum_{\tau=-W_{len}}^{\tau=+W_{len}} \left|W_X((t-\tau),F_n) * W_y((t-\tau),F_n)\right|^2}}{\sqrt{\sum_{\tau=-W_{len}}^{\tau=+W_{len}} |W_X((t-\tau),F_n)|^2} \sqrt{\sum_{\tau=-W_{len}}^{\tau=+W_{len}} |W_Y((t-\tau),F_n)|^2}} \tag{4}$$

We used WCC5.exe (see above) to compute Eq. (4) for all scales for a selected sample of data at any given time point in an ECoG file saved in EDF. WCC5.exe allows the constants in Eqs. (1) and (2) to be changed as desired so that different wavelets can be studied.

As noted above, the clinical stimulations sometimes cause ADs which were then treated by the clinical team with brief pulse stimulation (Lesser et al., 1999) and/or a cognitive task in attempt to stop the ADs. Wavelet cross-coherence was calculated for two short sections of ECoG during these ADs. The first section, referred to as E1, was taken after the AD had started but before the cognitive task was given. As also described above, the cognitive task consisted of the patients being asked to answer an arithmetic or spelling question. The second section, referred to as E2, was taken while the patient thought about and answered the question. As in our previous paper (Lesser et al., 1999) if the ADs stopped during or within 2 s after the end of the cognitive task, without further intervention, it was treated as success and the trial was scored as M1. If ADs continued for more than two seconds after the end of the answer, the trial was treated as failed and scored as M0. ADs were continuously present in the E1 sections, and the E1 section ended before the question for the cognitive task started. Arithmetic or spelling task sections occurred after the end of the E1 sections, and always were initiated while ADs were present.

As noted, the clinical team used brief pulses of stimulation to stop ADs. We only selected trials where we could obtain 4 s periods for both E1 and E2 that did not contain any brief pulses of stimulation. Some trials where the cognitive task was delivered could also contain several closely spaced brief pulses of stimulation that would terminate the AD. In such cases it was not possible to obtain clear 4 s sections of AD recording. On the other hand, some ADs continued for several seconds and gave the opportunity for more than one cognitive task. In these cases, an E1 section was selected after the AD had started but before the first cognitive task question and answer. The first E2 section was chosen during the first cognitive task and was fully contained by this cognitive task. There was a pause after which a second cognitive task was given to the patient. A second arithmetic or spelling task (E2) section was collected and fully contained in this second cognitive task. The first arithmetic or spelling task section was scored as M0, failed. The second section could be either scored M0 (did not stop ADs) or scored M1 (ADs stopped) depending on whether the ADs stopped within 2 s (Lesser et al., 1999).

The first step to computing wavelet cross-coherence was to apply Eq. (2) to the 4 s period to each member of a given pair of electrodes. Next Eq. (4) was computed for these two 4.0 s periods to produce the value of wavelet cross-coherence for each pair of electrodes. This process was repeated for all pairs for each E1 and arithmetic or spelling task periods.

In order to observe overall change in coherence we evaluated changes in the mean wavelet cross-coherence for all electrode pairs, comparing results in the E2 sections to those in the E1 sections. We also determined whether, during the E2 section, ADs stopped (M1)

or did not stop (M0). A decrease in mean wavelet cross-coherence in the E2 sections compared to mean values in the E1 sections would indicate that activity had decreased in the specific frequency range. We performed all these calculations for each of the 19 frequencies that covered the range of our data from 1.69 Hz to 300 Hz. This way we could detect in which frequency range these changes in activity occurred. Since the wavelet frequencies overlap to some extent, there are no gaps in coverage in the frequency ranges used in this study. wavelet cross-coherence values are always in the range 0.0 to 1.0 due to the normalization denominator term in Eq. (4).

2.7. Statistical analysis

For each patient, trial, and frequency, we calculated the mean wavelet cross-coherence over all electrode pairs and calculated the change in the mean after versus before the arithmetic or spelling task. We calculated 95% confidence intervals for the means and changes in means using robust variance estimates (Reid and Crépeau, 1985; Lin, 1989) that account for correlation among multiple trials within patients. We graphed the percentage of trials for which the ADs stopped when the mean increased vs. when the mean decreased by frequency (Fig. 3).

To evaluate whether the change in the mean coherence is associated with the success of the cognitive task in stopping ADs, we used mixed-effects logistic regression to model the probability of the AD stopping as a function of the change in mean coherence. We included the patient as a random effect to account for correlation among multiple trials for the same patient. To protect against multiple comparisons, we first tested for an interaction between the change and the frequency. Given that this interaction was highly significant (F-test value [df = 18, 2152] = 2.01, p = 0.0069), we went on to fit separate models by frequency. As sensitivity analyses, we refit the model restricting to electrode pairs where at least one electrode had an AD, where exactly one electrode had an AD, where both electrodes had an AD, and where no electrodes had an AD. Additional sensitivity analyses included the following: One adjusted for the potential confounding variables of patient age, patient gender, and side of implantation and testing. A second, adjusted for the potential confounding variables of number of electrode pairs with ADs, AD morphology, intensity of stimulation, and duration of stimulation. A third adjusted for baseline wavelet cross-coherence. All statistical tests are two-sided with an alpha of 0.05. Data were analyzed with SAS 9.4.

We used the Cochran-Mantel-Haenszel chi-square test to adjust for correlation among multiple trials within the same patients while testing whether ADs were more likely to stop when AST and BPS were used together, or when either one was used alone.

2.8. Functional MRI data processing

fMRI data were processed using SPM12 software (http://www.fil.ion.ucl.ac.uk/spm/) implemented in MATLAB R2014b (MathWorks, Natick, MA 01760 USA). The General Linear Model (GLM) was utilized for mapping brain activation both at single subject and group level.

For initial data pre-processing, fMRI raw data were slice-time corrected, spatially realigned to correct for head motion, normalized to MNI space at 2 mm voxel resolution, and spatially smoothed using a 6 mm isotropic full width at half maximum (FWHM) Gaussian filter.

From the pre-processed fMRI raw data, activation maps were generated through use of the General Linear Model analysis within SPM12 by convolving the stimulus corresponding to each paradigm with a standard canonical gamma hemodynamic response function (HRF), with display as T-statistic maps overlaid on T1 weighted 3D MPRAGE anatomic images.

For the arithmetic processing task, we examined "simple" computation vs. rest, and "difficult" computation vs. rest. For spelling, we examined forward spelling vs. rest and backward spelling vs. rest. We found similar topography of activation on the simple and difficult versions of the tasks but with slightly increased intensity/robustness of activation with the difficult versions. Hence, results from the simple tasks are not reported here.

Control subject data were analyzed at both single subject and group levels, and the group level analysis was used to provide normative data for each paradigm to enable us to effectively analyze the patient's data at a single subject level. We found similar topographies of activation on the simple and difficult versions of the tasks but with slightly increased intensity/robustness of activation with the difficult versions. Therefore, we only report the results of the difficult versions in this paper. Evaluation of the topography of activation on the control subject group-averaged activation maps was the main basis for selection of appropriate statistical thresholds for individual patient activation maps. The individual patient activation maps were subjectively individually thresholded to highlight activation in the eloquent areas demonstrated on the group-averaged control activation maps while minimizing noise-related spurious activation elsewhere in the brain.

Note that at times there are apparent activation outside of the anatomical location of brain. Such findings are thought due to a combination of things: functional (BOLD EPI)-anatomic misregistration; spurious activation related to large draining veins both in the meninges and within diploic space and particularly scalp; motion artifacts related to bulk head rotational and translational motion; and in cases near the base of the brain, physiologic artifacts related to factors such as swallowing, eye motion or excessive blinking, or cardiorespiratory/cerebrospinal fluid pulsation. These are well-known confounds in functional imaging, and regression of these is often part of resting state fMRI preprocessing steps, but for task fMRI we generally don't use such preprocessing steps routinely, and we did not do so for these studies. We also did not use a mask to exclude spurious extracranial (e.g., scalp) activation.

2.9. fMRI surface reconstruction

We performed surface reconstructions of the images obtained from the complex computation paradigm. The anatomical MRI (MPRAGE) images co-registered to the fMRI data were automatically segmented using MRICloud (www.mricloud.org) (Mori, 2016) pipeline to define the brain surface. The surface rendering and superimposition of fMRI activation maps were performed using Amira (FEI, Hillsboro, Oregon, USA).

Three types of surface mesh files were created using Amira; the brain surface, the cortex-white matter boundary, and the fMRI activation sites. The former two surface definitions were generated from the segmentation of the MPRAGE images performed by MRICloud. Subject specific thresholding was used, since no fixed threshold could be applied to all subjects. Individual patient thresholds were selected based on expected topography of activation, using group-averaged normal control activation maps as a reference standard for each paradigm. For the three-dimensional visualization, the three surface meshes were displayed simultaneously while the outer-most surface (the brain surface) had an opacity level at 0.5 to visualize the activation sites inside the brain.

3. Results

3.1. Effect of an arithmetic or spelling task (AST) on afterdischarges

Recording from 1276 implanted electrodes among 15 patients, an AST (examples: "what is 43 − 17?", "spell 'house' backwards")

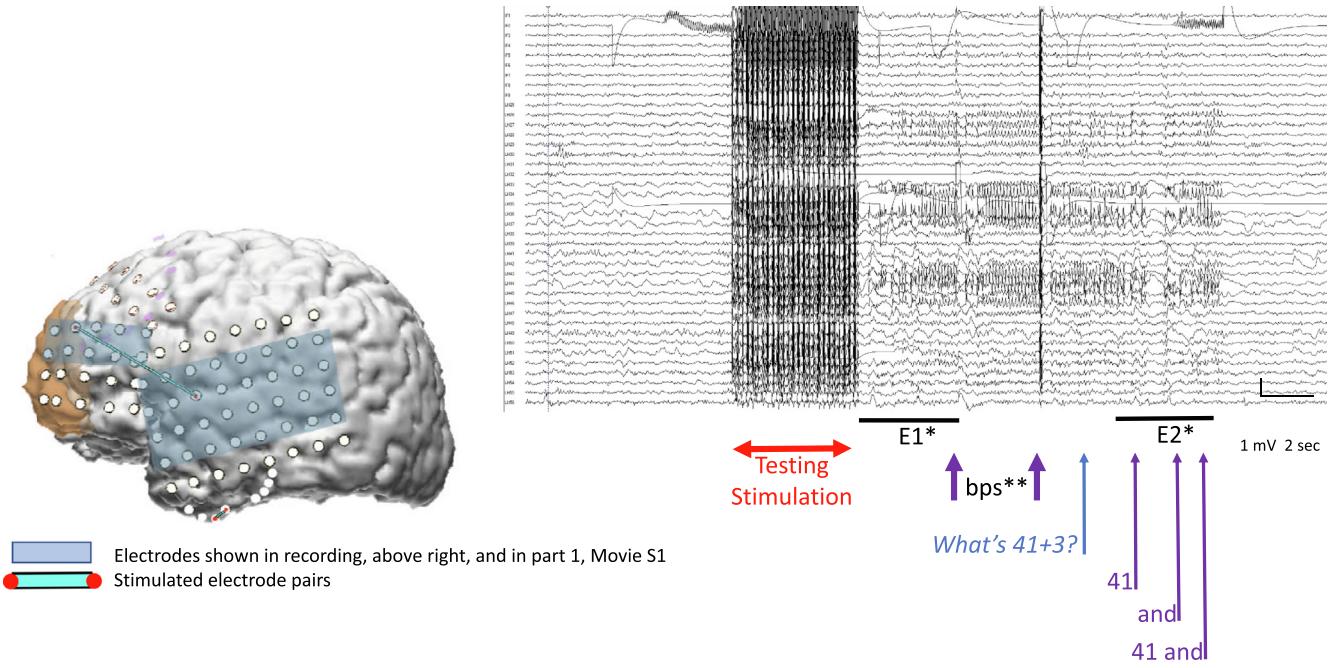

Fig. 3. Effects on ADs with stimulation and with an arithmetic question. Electrode pairs are stimulated during clinical testing. We analyzed two 4000 msec periods, the first occurred before an arithmetic or spelling task had been given. We call this *__E1__ – indicating the first analyzed four second epoch. The second began after the tester had begun to state the arithmetic or spelling problem. We call this *__E2__ – indicating the second analyzed four second epoch. (See Supplemental Figs. S1–S3). The brain image on the left shows the two pairs that were stimulated (blue lines, a longer one going from frontal to temporal region, and a shorter one at the temporal base). Electrocorticography recording (ECoG) is shown on the right for the event that occurred with stimulation of the pair of electrodes indicated by the top blue line. Electrodes shown on ECoG are highlighted with the light blue rectangular box. The horizontal double arrow indicates when clinical stimulation occurred. Next two shorter vertical pink lines indicate when brief pulses of stimulation (**__bps__) were administered in an attempt to end the afterdischarges. Because they did not stop, an arithmetic question was asked, "What's 41 + 3?" The onset of the question is indicated by the blue arrow. The patient answers "41. . . and. . . 41 and". The onset of each portion of her reply is likewise indicated by an arrow. Supplemental Movie S1 shows what occurred with this, and with another occurrence with testing at the electrodes indicated by the lower blue line in the image on the left. In the other trial in Supplemental Movie S1 the patient was first asked "What's 34 + 5?" and when she answered 39 was then asked, "minus 12?". Supplemental Movie S2 shows another patient who is asked "What's 50 – 12?" He answers 38 and is then asked "38 times 2." In both of these additional examples the ADs did not stop in response to the first question but did stop after the second question. Calibration indicates 1 milivolts, and 2 s. See Supplemental Figs. S1–S3 for further details.

was successful in stopping ADs in 50 of 116 trials. (Fig. 3, Supplemental Table 1, Supplemental Figs. S1–S3, and Supplemental Movies S1 and S2.) We entered responses to the clinical testing on MRI/CT reconstructions of the implanted electrode locations with respect to the underlying brain. On the same reconstructions, we depicted the sites at which an AST had been used to stop ADs and noted whether the attempts had been successful or unsuccessful in stopping them. (Supplemental Figs. S4–S21.)

Termination of ADs could occur with testing in either hemisphere, could occur whether or not ADs had been preceded by BPS, whether or not the site with ADs also was a site of seizure onset, and whether or not the ADs were in a region thought important for arithmetic or spelling (Morris et al., 1984; Lesser et al., 1986; Whalen et al., 1997; Duffau et al., 2002; Bitan et al., 2005; Philipose et al., 2007; Dastjerdi et al., 2013) (Fig. 4).

We found that AST and BPS succeeded in ending ADs 57% and 59% of the time respectively when each was used alone, whereas they succeed 37% of the time when used together. These results did not reach statistical significance. (Cochran-Mantel-Haenszel chi-square test, Supplemental Table 2; see Supplemental Table 1 for results on individual patients.)

3.2. fMRI activation with ASTs

Six patients returned for fMRI localization of sites activated during ASTs. In these patients, and nine controls, we found activated regions throughout the brain, many of which are known to participate in control of mental effort (Shenhav et al., 2017) (Supplemental Tables 1 and 3).

Although the sites activated during fMRI testing could overlap with those where ADs had been terminated by ASTs, the two did not necessarily correspond. This was the case when comparing AST results to fMRI results both in the same patient and in the controls. (Fig. 4 and Supplemental Figs. S22–43).

3.3. Coherence measurements

We measured wavelet cross-coherence (**WxCoh**) among all the implanted electrodes during AD occurrence, measuring all possible pair combinations, regardless of whether ADs had occurred at individual electrodes within a given pair. We measured a 4000 msec period before an AST had been given and a 4000 msec period beginning after the tester had begun to state the AST problem. We calculated WxCoh before the AST and also calculated WxCoh beginning when the AST was given.

We examined the mean WxCoh among channel pairs prior to the AST (Supplemental Table 4). We found that the mean baseline WxCoh was significantly higher in the lowest (1.69–5.35 Hz) frequency ranges among channels pairs for which one or both channels had ADs during trials when ADs subsequently stopped versus trials when ADs did not subsequently stop.

We also evaluated the changes occurring before versus after the ASTs began, comparing findings when ADs stopped versus when ADs did not stop. We found that ADs were significantly more likely to stop when WxCoh decreased within the beta, alpha, and theta bands (Fig. 5), with significant p-values with respect to the peak frequency of each wavelet scale frequency response as follows: 7.13 Hz $p = 0.035$, 9.5 Hz $p = 0.001$, 12.67 Hz $p = 0.010$, 16.89 Hz

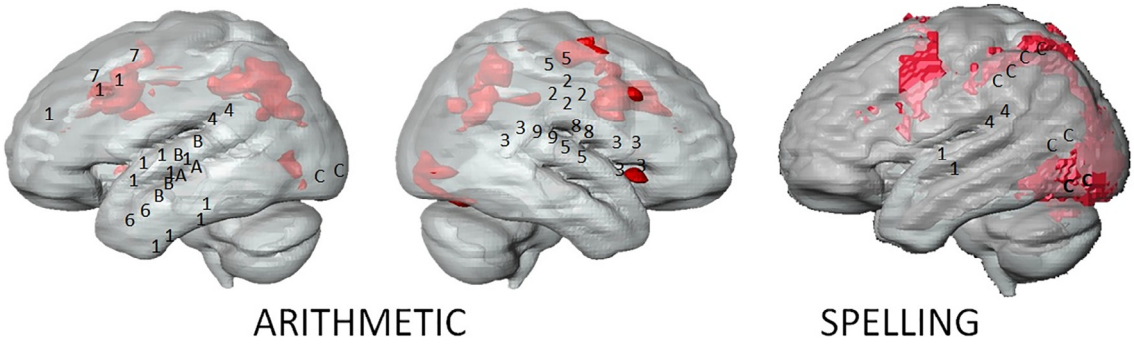

Fig. 4. Locations where cognitive effort (arithmetic or spelling tasks) was followed by ending of afterdischarges, superimposed on summary sagittal surface-rendered 3D fMRI image displays of the locations activated by arithmetic or spelling tasks in 9 controls. Numbers 1–9 indicate the patients 1–9; A is patient S11, B patient S12, C patient S14. AST did not end the ADs in patients S10, S13 and S15. The left two images show findings with arithmetic tasks during left and right brain stimulation, respectively. The right image shows findings with spelling tasks during left brain stimulation. Spelling was not used with right brain testing.

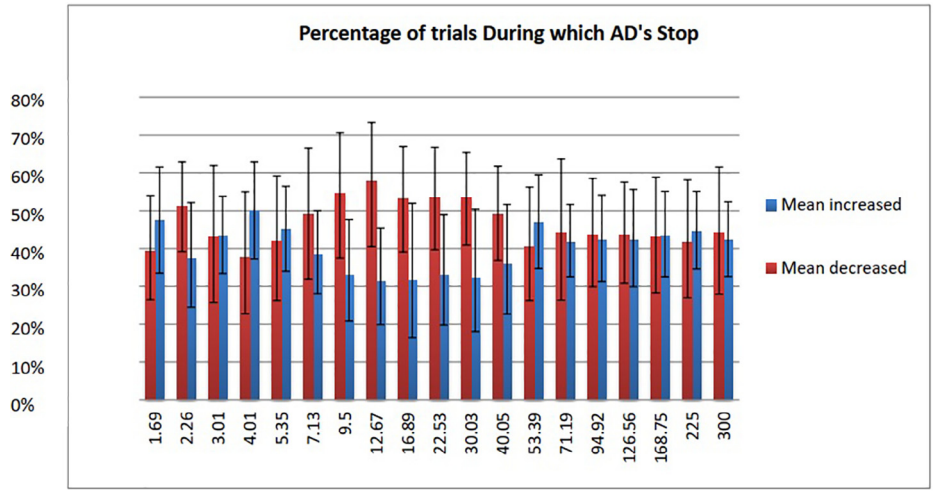

Fig. 5. Percentage of trials during which ADs stopped with respect to whether the mean wavelet cross-coherence of electrode pairs increased or decreased at each frequency. Error bars represent 95% confidence intervals for the percentages. When there was a decrease in the mean coherence in the beta, alpha, and high theta ranges, ADs were more likely to stop.

p = 0.008, 22.53 Hz p = 0.034 (Supplemental Table 5). There were no systematic changes in WxCoh in the lowest frequencies when comparing results before to those after onset of the ASTs.

Adjusting for the baseline WxCoh in a sensitivity analysis (Supplemental Table 6) did not change the significance of associations shown in Fig. 5, the association between decreases in WxCoh after vs. before the AST, and the probability of the ADs stopping. The finding that ADs were significantly more likely to stop when WxCoh decreased within the beta, alpha, and theta bands remained true for most bands and conditions when restricting AD pairs analyzed to those with ADs in one channel, in both channels, or in neither channel. This remained true after adjusting for patient age and gender, and side of testing, and after adjusting for number of electrodes with ADs, AD morphology, intensity of stimulation, and duration of stimulation.

4. Discussion

4.1. Non-invasive modification of seizure activity

Somatosensory stimulation or motor activity of a limb can abort focal seizures in that limb (Gowers, 1881; Efron, 1956; Wolf, 2002): these have been used since at least the second century (Gowers, 1881). With these, blocking of brain activity is by a specific behavior, affecting a brain region important for the behavior and in which the seizure is originating. (Gowers, 1881; Efron, 1956; Wolf, 2002). However, epileptiform activity can be modified in at least some patients with generalized seizures (Beniczky et al., 2012; Lunardi et al., 2016).

Operant conditioning, biofeedback, relaxation therapies, and other behavioral methods can reduce seizures and can alter EEG or evoked potential activity (Efron, 1957; Sterman et al., 1974; Sterman and Shouse, 1980; Kotchoubey et al., 2001; Nagai et al., 2004; Fumuro et al., 2013; Kotwas et al., 2016, Fumuro et al., 2018). These take time to learn, and often several training sessions, whereas our patients' ADs were terminated quickly, and without prior training. Moreover, the patients we describe experienced the tasks as not relaxing but stressful, and stress can increase seizure occurrence (Temkin and Davis, 1984; Kotwas et al., 2016). Similarly, tastes and smells can abort seizures, but this may be more likely if they are unpleasant (Gowers, 1881; Efron, 1956). Taken together, these findings suggest that, although stress can be accompanied by increased seizures in some circumstances, in others, circumscribed stress can increase the effectiveness of the methods we used to abort impending seizures. The ability of these methods to terminate seizures, may relate to the intensity of arousal or mental effort during these brief periods of time (Efron, 1957; Beniczky et al., 2012; Kotwas et al., 2016; Lunardi et al., 2016).

In our patients, the success of AST (57%) and BPS (59%) was similar when each was used alone. The decreased effectiveness (37%)

when the two were used together raises the possibility that they might interfere with one another, but also could occur because they were used together when ADs were more resistant to termination. However, the results did not reach statistical significance.

4.2. Cortical location of regions modulating arithmetic and spelling

Were the ADs in regions modulating arithmetic or spelling, so that ASTs "competed" with the processes generating ADs and won? We and others have demonstrated the presence of areas participating in arithmetic function in the posterior and inferior temporal lobe, the parietal lobe, the frontal lobes, and the thalamus (Ojemann, 1974; Morris et al., 1984; Lesser et al., 1986; Whalen et al., 1997; Duffau et al., 2002; Dastjerdi et al., 2013; Daitch et al., 2016; Pinheiro-Chagas et al., 2018). Spelling has been localized to the temporal lobe (including superior temporal gyrus and posterior inferior temporal lobe), parietal lobe (including supramarginal and angular gyri and intraparietal sulcus), and inferior frontal lobe (Morris et al., 1984; Bitan et al., 2005; Philipose et al., 2007). However, in the patients we studied, the arithmetic and spelling tasks could stop ADs generated by stimulated electrode pairs located throughout the brain, and whether or not they occurred in regions important for calculation or spelling. Therefore, localization by itself doesn't explain our results. It is possible that the patients' operations resulted in re-organization of regions important for the arithmetic and spelling tasks. However, regions that were resected for treatment of a patient's seizures did not particularly correspond to regions activated by AST on fMRI either in patients or controls, so resections are unlikely to have affected the fMRI localizations in our patients, and of course did not occur in the controls (Fig. 4, Supplemental Figs. S22–S43).

4.3. Frequency ranges and associated cortical changes

We previously studied activity in the 70–110 Hz (gamma) range (Muldoon et al., 2018) and found that AD suppression was more likely when sites with ADs co-localized with a stable, coherent functional network. This is consistent with the idea that gamma activity reflects relatively localized cortical activity (Kopell et al., 2000; Kopell et al., 2014; Khambhati et al., 2016). The changes observed could be conceptualized as due to alteration of a small-world network (Netoff et al., 2004; Ponten et al., 2007) with changes in the strength of connections, interactions, and integration within the network; to changes in non-linear, deterministic connections within the network (Lehnertz, 2008; Frei et al., 2010; Quan et al., 2011), with consequent disruption of an attractor state (Thompson and Varela, 2001; Le Van Quyen et al., 2003); or to altered synchronization or propagation (Ponten et al., 2007; Sauseng et al., 2007; Schindler et al., 2008; Kalamangalam et al., 2014).

Our previous report assessed the gamma frequency range using network analysis tools, whereas in this report we examined all recorded frequencies and assessed coherence. In the current study we show significant findings in lower frequency bands. Our two reports, taken together, support the idea that multiple mechanisms might simultaneously underlie specific behaviors. The temporal relationship (Asano et al., 2013) between the ECoG changes and the cessation of afterdischarges supports the idea that the tasks used were causally related to widespread brain changes that in turn resulted in termination of afterdischarges.

When the cognitive tasks were successful in terminating the ADs, there was increased delta coherence at baseline with no significant change during the tasks. Increases in delta power and synchrony have been associated with increased attention, concentration, and during decision making (Knyazev, 2012; Nacher et al., 2013; Kopell et al., 2014), including during arithmetic tasks (Dimitriadis et al., 2010; Harmony, 2013; Zarjam et al., 2013)

In addition, when ADs terminated in our patients, coherence decreases in the beta, alpha, and theta frequency ranges occurred throughout the brain. This is consistent with the previous finding that these rhythms can reflect interactions between structures that are more distant from one another than, for example, those whose interactions are reflected by gamma activity. (Crone et al., 1998; Kopell et al., 2000; Donner and Siegel, 2011; Klimesch, 2012; Khambhati et al., 2016; Helfrich et al., 2018; Zhang et al., 2018) Coherence decreases in the high alpha range can reflect attentional mechanisms (Klimesch, 2012). Attenuation of alpha and beta activity have both been associated with changes in attention and voluntary activity (Engel and Fries, 2010; Klimesch, 2012; Meirovitch et al., 2015; Abel et al., 2016), with active processing (Miller et al., 2012; Fonken et al., 2016), with increased brain excitation (Palva and Palva, 2011; Meirovitch et al., 2015), attenuation of beta activity with the occurrence of a novel or unexpected event (Engel and Fries, 2010), attenuation of alpha activity with increased memory load (Crespo-Garcia et al., 2013) and of theta activity with increased decision time and with attentional modulation (Caplan et al., 2001; Spyropoulos et al., 2018). Among the patients we report here, activity attenuation seemed to reflect diffuse cortical changes, occurring in response to the cognitive tasks (Pfurtscheller, 2006). Our findings also are consistent with the evidence that widespread desynchronization can result in alterations of focal brain activity (Engel and Fries, 2010; Siegel et al., 2012), with the mental effort resulting in to top-down modulation of attention and cognition, and in widespread changes in synchronization, including within the cortex generating the ADs.

In summary, the previous literature indicates that important changes occur in lower frequency ranges in response to cognitive tasks. The details of the changes may depend on the details of the tasks.

4.4. Local responses to diffuse brain changes

Several studies have shown that surrounding brain importantly interacts with seizure onset zones to enhance or diminish likelihood of seizure spread, (Jiruska et al., 2013; Khambhati et al., 2016) or of seizure persistence after seizure surgery (Tomlinson et al., 2017). In our patients, fMRI indicated that ASTs activated cerebral regions which have been implicated in the exertion of cognitive effort (Shenhav et al., 2017), but which did not necessarily include or surround areas of epileptogenesis. We hypothesize that the activation secondarily caused desynchronization of activity throughout the cortex, including areas with ADs, so that the ADs stopped. We found inter-electrode coherence changes occurred regardless of location and regardless of the amount of separation between electrode pairs. This could occur if the areas initially activated by ASTs altered activity in subcortical nuclei (Kopell et al., 2014) which then altered cortical activity broadly. We previously have shown that ADs can vary in occurrence and distribution from one stimulation trial to the next (Lesser et al., 2008). Thus, the other possibility is that there could be a latent widespread network within the cortex itself which can be activated, deactivated, or modified in circumstances such as we evaluated. Taken together, these findings suggest that possibly subtle changes in activity, attention, and cognition during ASTs affected activity diffusely that in turn made it more likely that ADs would stop locally in response to ASTs.

4.5. Local mechanisms underlying activity changes

Beta and alpha activity are thought to be generated in the cortical pyramidal cell layer (Roopun et al., 2006; Engel and Fries,

2010; Klimesch, 2012). We speculate that ASTs modified the excitability of slow-inhibitory interneurons (Frei et al., 2010; Kalamangalam et al., 2014; Kopell et al., 2014), which in turn altered activity in pyramidal cells that otherwise might have continued to generate ADs. Cortical responses to ASTs might also constitute noise with respect to the AD network, driving the network out of equilibrium (Deco et al., 2011). If the responses constituted noise, it also is possible that ADs were disrupted because signal to noise ratios were no longer sufficient to maintain the network. Related to this are observations that small changes in extracellular field potentials can alter neuronal firing, and thus disrupt local synchronous activity (Anastassiou et al., 2011). These would help to explain why AD suppression was more likely in these patients when the ADs were part of a stable, coherent network (Muldoon et al., 2018): disruption of coherence throughout the brain included disrupted coherence within the previously stable network so that AD activity stopped. Further work would be needed to determine precisely what tasks and circumstances would make this most likely. In this study we looked only at within frequency coherence, but study of cross frequency interactions might provide further insights into the phenomena we observed.

4.6. Clinical implications

We only could record where electrodes had been placed, and only studied 15 patients, but there are in any case differences both among and within patients (Blume et al., 2004; Freestone et al., 2017; Bansal et al., 2018; Maharathi et al., 2018; Marino et al., 2018) so that we do not expect that one mechanism would explain all patients or all seizures. However, a strength of this study is that we were able to record from electrodes that were placed at sites, and cognitive effort could terminate ADs at sites, located widely throughout the cortex (Fig. 4). Therefore, our findings are unlikely to pertain only to specific brain regions. There are differences of opinion regarding the relationship between ADs, the seizure onset zone, and clinical seizures (Blume et al., 2004; Trevelyan et al., 2007; David et al., 2010; Kalamangalam et al., 2014), but under at least some circumstances, the ADs and seizures respond similarly. For example, brief stimulation pulses such as we report here can terminate ADs (Lesser et al., 1999), and brief stimulation pulses are used in a device to terminate clinical seizures (Morrell, 2011).

Our findings may help explain why methods such as vagal nerve and deep brain stimulation which have widespread effects can help control seizures originating in restricted regions. The effects of cognitive effort or of stimulation may be widespread, but enough to disrupt local synchronized activity: the whole is stronger than the part. Our findings also are consistent with the suggestion that the effectiveness of local stimulation might be the result of indirect modulation rather than a direct effect at the stimulation site (Kokkinos et al., 2019). In addition, focal seizures may increase epileptogenicity throughout the brain (Sheybani et al., 2018), and pan-cerebral methods such as described here could help in modifying this activity There has been considerable recent progress in developing external devices which could indicate seizure occurrence, but these so far are most sensitive to motor manifestations of convulsions (Kotwas et al., 2016; Krauss and Ryvlin, 2018). However, there may be other changes outside the brain that could predict likely occurrence of seizure, regardless of seizure type (Kotwas et al., 2016; Kuhlmann et al., 2018). Detected changes could then trigger presentation on an external device of an arithmetic, spelling, or other item for the patient to consider or solve. Doing this could result in changed brain activity, including arrest of seizure discharges in the epileptogenic region. Similar interventions might be possible for other neurological disorders.

Acknowledgements

Rebecca Fisher, Karen George, Viktar Kanasevich, and Noelle Stewart performed clinical stimulation testing, Nathan Crone directed clinical CT/MRI reconstructions, and advised regarding use of Photoshop to annotate the reconstructions. Cameron Davis and Mel Gross in the Argye Hillis lab performed neglect testing. Joe Gillen assembled test sequences for, and Terri Brawner, Kathleen Kahl, and Ivana Kusevic performed, the fMRI evaluations. We thank Danielle Bassett, Dana Boatman, Nathan Crone, Nancy Kopell, Sarah Muldoon, Amir-Homayoon Najmi, Bill Sutherling, and Roger Traub for discussions, and thank the patients and controls who came for the fMRI studies.

Author contributions

RPL conceived the AST paradigms for the clinical evaluations and fMRI studies, participated in assessing and marking ECoG recordings, instructed subjects regarding and was present for fMRI studies, analyzed the data and wrote the paper, together with WRSW and DLM. WRSW participated in and directed assessment and marking of ECoG recordings, developed the software for viewing, and participated in marking, the ECoG, carried out waveform and coherence analyses. SC, AL and HJL participated in marking the ECoG recordings. DLM performed statistical analyses of the results. PFM cared for the initial patient. JJP participated in developing the fMRI paradigms. JJP and SA analyzed the fMRI recordings. SM performed fMRI reconstructions. All co-authors reviewed the manuscript. RPL and JJP are co-senior authors for this manuscript.

Funding

The study was funded by gifts from patients and their families.

Declaration of Competing Interest

Dr. Lesser or his wife has stock in the following companies which sell health care products: Abbott Labs, Abbvie, Apple, Avanos, Celgene, Express Scripts, Johnson and Johnson, Merck & Company, Pfizer. These have been disclosed to and approved by the Johns Hopkins University in accordance with its conflict of interest policies. Dr. Mori is the partial owner and CEO of AnatomyWorks. This arrangement has been reviewed and approved by the Johns Hopkins University in accordance with its conflict of interest policies. Under a license agreement between AnatomyWorks and the Johns Hopkins University, Dr. Mori and the University are entitled to royalty distributions related to the brain segmentation technology described in the study. The other authors report no conflicts.

Appendix A. Supplementary material

Supplementary data to this article can be found online at https://doi.org/10.1016/j.clinph.2019.07.007.

References

Abel TJ, Rhone AE, Nourski KV, Ando TK, Oya H, Kovach CK, et al. Beta modulation reflects name retrieval in the human anterior temporal lobe: an intracranial recording study. J Neurophysiol 2016;115(6):3052–61.
Asano E, Brown EC, Juhasz C. How to establish causality in epilepsy surgery. Brain Dev 2013;35(8):706–20.
Anastassiou CA, Perin R, Markram H, Koch C. Ephaptic coupling of cortical neurons. NatNeurosci 2011;14(2):217–23.
Bansal K, Nakuci J, Muldoon SF. Personalized brain network models for assessing structure-function relationships. Curr Opin Neurobiol 2018;52:42–7.
Beniczky S, Guaranha MS, Conradsen I, Singh MB, Rutar V, Lorber B, et al. Modulation of epileptiform EEG discharges in juvenile myoclonic epilepsy: an investigation of reflex epileptic traits. Epilepsia 2012;53(5):832–9.

Bitan T, Booth JR, Choy J, Burman DD, Gitelman DR, Mesulam MM. Shifts of effective connectivity within a language network during rhyming and spelling. J Neurosci 2005;25:5397–403.

Blume WT, Jones DC, Pathak P. Properties of after-discharges from cortical electrical stimulation in focal epilepsies. Clin Neurophysiol 2004;115:982–9.

Bruns A. Fourier-, Hilbert- and wavelet-based signal analysis: are they really different approaches? J Neurosci Methods 2004;137:321–32.

Caplan JB, Madsen JR, Raghavachari S, Kahana MJ. Distinct patterns of brain oscillations underlie two basic parameters of human maze learning. J Neurophysiol 2001;86(1):368–80.

Crespo-Garcia M, Pinal D, Cantero JL, Diaz F, Zurron M, Atienza M. Working memory processes are mediated by local and long-range synchronization of alpha oscillations. J Cogn Neurosci 2013;25(8):1343–57.

Crone NE, Miglioretti DL, Gordon B, Lesser RP. Functional mapping of human sensorimotor cortex with electrocorticographic spectral analysis. II. Event-related synchronization in the gamma band. Brain 1998;121:2301–15.

Lin DY, LTW. The Robust Inference for the Cox Proportonal Hazards Model. J Amer Stat Assoc 1989;84(408):1074–8.

Daitch AL, Foster BL, Schrouff J, Rangarajan V, Kasikci I, Gattas S, et al. Mapping human temporal and parietal neuronal population activity and functional coupling during mathematical cognition. Proc Natl Acad Sci USA 2016;113:E7277–86.

Dastjerdi M, Ozker M, Foster BL, Rangarajan V, Parvizi J. Numerical processing in the human parietal cortex during experimental and natural conditions. Nature Commun 2013;4:2528.

David O, Bastin J, Chabardes S, Minotti L, Kahane P. Studying network mechanisms using intracranial stimulation in epileptic patients. Front Syst Neurosci 2010;4:148.

Deco G, Jirsa VK, McIntosh AR. Emerging concepts for the dynamical organization of resting-state activity in the brain. Nat Rev Neurosci 2011;12(1):43–56.

Dimitriadis SI, Laskaris NA, Tsirka V, Vourkas M, Micheloyannis S. What does delta band tell us about cognitive processes: a mental calculation study. Neurosci Lett 2010;483(1):11–5.

Donner TH, Siegel M. A framework for local cortical oscillation patterns. Trends Cogn Sci 2011;15(5):191–9.

Duffau H, Capelle L, Lopes M, Bitar A. Sichez JP, Van Effenterre R. Medically intractable epilepsy from insular low-grade gliomas: improvement after an extended lesionectomy. Acta Neurochir(Wien) 2002;144:563–72.

Efron R. The effect of olfactory stimuli in arresting uncinate fits. Brain 1956;79(2):267–81.

Efron R. The conditioned inhibition of uncinate fits. Brain 1957;80:251–62.

Engel AK, Fries P. Beta-band oscillations–signalling the status quo? Curr Opin Neurobiol 2010;20(2):156–65.

Fonken YM, Rieger JW, Tzvi E, Crone NE, Chang E, Parvizi J, et al. Frontal and motor cortex contributions to response inhibition: evidence from electrocorticography. J Neurophysiol 2016;115(4):2224–36.

Freestone DR, Karoly PJ, Cook MJ. A forward-looking review of seizure prediction. Curr Opin Neurol 2017;30(2):167–73.

Frei MG, Zaveri HP, Arthurs S, Bergey GK, Jouny CC, Lehnertz K, et al. Controversies in epilepsy: debates held during the Fourth International Workshop on Seizure Prediction. Epilepsy Behav 2010;19:4–16.

Fumuro T, Matsuhashi M, Matsumoto R, Usami K, Shimotake A, Kunieda T, et al. Do scalp-recorded slow potentials during neuro-feedback training reflect the cortical activity? Clin Neurophysiol 2018;129(9):1884–90.

Fumuro T, Matsuhashi M, Mitsueda T, Inouchi M, Hitomi T, Nakagawa T, et al. Bereitschaftspotential augmentation by neuro-feedback training in Parkinson's disease. Clin Neurophysiol. 2013;124(7):1398–405.

Gooneratne IK, Green AL, Dugan P, Sen A, Franzini A, Aziz T, et al. Comparing neurostimulation technologies in refractory focal-onset epilepsy. J Neurol Neurosurg Psychiat 2016;87(11):1174–82.

Gowers WR. Epilepsy and other chronic convulsive diseases: their causes, symptoms, and treatment. London: J & A Churchill; 1881. Pages 93–97, 288–289

Hamberger MJ, Goodman RR, Perrine K, Tamny T. Anatomic dissociation of auditory and visual naming in the lateral temporal cortex. Neurology 2001;56:56–61.

Harmony T. The functional significance of delta oscillations in cognitive processing. Front Integrative Neurosci 2013;7:83.

Helfrich RF, Fiebelkorn IC, Szczepanski SM, Lin JJ, Parvizi J, Knight RT, et al. Neural mechanisms of sustained attention are rhythmic. Neuron 2018;99(4). 854-65.e5.

Jiruska P, de Curtis M, Jefferys JG, Schevon CA, Schiff SJ, Schindler K. Synchronization and desynchronization in epilepsy: controversies and hypotheses. J Physiol 2013;591(4):787–97.

Kalamangalam GP, Tandon N, Slater JD. Dynamic mechanisms underlying afterdischarge: a human subdural recording study. Clin Neurophysiol 2014;125(7):1324–38.

Kemp B, Varri A, Rosa AC, Nielsen KD, Gade J. A simple format for exchange of digitized polygraphic recordings. Electroenceph Clin Neurophysiol 1992;82(5):391–3.

Khambhati AN, Davis KA, Lucas TH, Litt B, Bassett DS. Virtual cortical resection reveals push-pull network control preceding seizure evolution. Neuron 2016;91(5):1170–82.

Klein A, Sauer T, Jedynak A, Skrandies W. Conventional and wavelet coherence applied to sensory-evoked electrical brain activity. IEEE Trans Biomed Eng 2006;53(2):266–72.

Klimesch W. alpha-band oscillations, attention, and controlled access to stored information. Trends Cogn Sci 2012;16(12):606–17.

Knyazev GG. EEG delta oscillations as a correlate of basic homeostatic and motivational processes. Neurosci Biobehav Rev 2012;36(1):677–95.

Kokkinos V, Sisterson ND, Wozny TA, Richardson RM. Association of closed-loop brain stimulation neurophysiological features with seizure control among patients with focal epilepsy. JAMA Neurol 2019;76:E1–9.

Kopell N, Ermentrout GB, Whittington MA, Traub RD. Gamma rhythms and beta rhythms have different synchronization properties. Proc Natl Acad Sci USA 2000;97:1867–72.

Kopell NJ, Gritton HJ, Whittington MA, Kramer MA. Beyond the connectome: the dynome. Neuron 2014;83(6):1319–28.

Kotchoubey B, Strehl U, Uhlmann C, Holzapfel S, Konig M, Froscher W, et al. Modification of slow cortical potentials in patients with refractory epilepsy: a controlled outcome study. Epilepsia 2001;42:406–16.

Kotwas I, McGonigal A, Trebuchon A, Bastien-Toniazzo M, Nagai Y, Bartolomei F, et al. Self-control of epileptic seizures by nonpharmacological strategies. Epilepsy Behav 2016;55:157–64.

Kovac S, Kahane P, Diehl B. Seizures induced by direct electrical cortical stimulation – mechanisms and clinical considerations. Clin Neurophysiol 2014;1:31-29.

Kramer MA, Eden UT, Lepage KQ, Kolaczyk ED, Bianchi MT, Cash SS. Emergence of persistent networks in long-term intracranial EEG recordings. J Neurosci 2011;31:15757–67.

Krauss GL, Ryvlin P. Non-EEG seizure detection is here. Neurology 2018;90(5):207–8.

Kuhlmann L, Lehnertz K, Richardson MP, Schelter B, Zaveri HP. Seizure prediction – ready for a new era. Nature Rev Neurol 2018;14(10):618–30.

Lachaux JP, Lutz A, Rudrauf D, Cosmelli D, Le Van QM, Martinerie J, et al. Estimating the time-course of coherence between single-trial brain signals: an introduction to wavelet coherence. Neurophysiol Clin 2002;32:157–74.

Le Van Quyen M, Navarro V, Martinerie J, Baulac M, Varela FJ. Toward a neurodynamical understanding of ictogenesis. Epilepsia 2003;44(Suppl 12):30–43.

Lehnertz K. Epilepsy and nonlinear dynamics. J Biol Phys 2008;34:253–66.

Lesser R, Gordon B, Uematsu S. Electrical Stimulation and Language. J Clin Neurophysiol 1994;11(2):191–204.

Lesser RP, Kim SH, Beyderman L, Miglioretti DL, Webber WRS, Bare M, et al. Brief bursts of pulse stimulation terminate afterdischarges caused by cortical stimulation. Neurology 1999;53:2073–81.

Lesser RP, Lee HW, Webber WR, Prince B, Crone NE, Miglioretti DL. Short-term variations in response distribution to cortical stimulation. Brain 2008;131:1528–39.

Lesser RP, Lüders H, Dinner DS, Klem G, Hahn JF, Harrison M. Electrical stimulation of Wernicke's area interferes with comprehension. Neurology 1986;36:658–63.

Lesser RP, Lüders H, Klem G, Dinner DS, Morris HH, Hahn J. Cortical afterdischarge and functional response thresholds: results of extraoperative testing. Epilepsia 1984;25:615–21.

Lesser RP, Lüders H, Klem G, Dinner DS, Morris HH, Hahn JF. Ipsilateral trigeminal sensory responses to cortical stimulation by subdural electrodes. Neurology 1985;35:1760–3.

Liu C, Yu T, Ren ZW, Xu CP, Wang XY, Qiao L, et al. Properties of afterdischarges from electrical stimulation in patients with epilepsy. Epilepsy Res 2017;137:39–44.

Lunardi MS, Lin K, Mameniskiene R, Beniczky S, Bogacz A, Braga P, et al. Olfactory stimulation induces delayed responses in epilepsy. Epilepsy Behav 2016;61:90–6.

Maharathi B, Wlodarski R, Bagla S, Asano E, Hua J, Patton J, et al. Interictal spike connectivity in human epileptic neocortex. Clin Neurophysiol 2018;130(2):270–9.

Marino AC, Yang GJ, Tyrtova E, Wu K, Zaveri HP, Farooque P, et al. Resting state connectivity in neocortical epilepsy: The epilepsy network as a patient-specific biomarker. Clin Neurophysiol 2018;130(2):280–8.

Martinet LE, Fiddyment G, Madsen JR, Eskandar EN, Truccolo W, Eden UT, et al. Human seizures couple across spatial scales through travelling wave dynamics. Nat Commun 2017;8:14896.

Meirovitch Y, Harris H, Dayan E, Arieli A, Flash T. Alpha and beta band event-related desynchronization reflects kinematic regularities. J Neurosci 2015;35(4):1627–37.

Miller KJ, Hermes D, Honey CJ, Hebb AO, Ramsey NF, Knight RT, et al. Human motor cortical activity is selectively phase-entrained on underlying rhythms. PLoS Comp Biol 2012;8(9) e1002655.

Mizuno-Matsumoto Y, Motamedi GK, Webber WR, Lesser RP. Wavelet-crosscorrelation analysis can help predict whether bursts of pulse stimulation will terminate afterdischarges. Clin Neurophysiol 2002;113:33–42.

Mori SW, Ceritoglu D, Li C, Kolasny Y, Vaillant A, Faria M, Oishi AV, Miller I, MI. MRICloud: delivering high-throughput MRI neuroinformatics as cloud-based software as a service. Comput Sci Eng 2016;18(5):21–35.

Morrell MJ. Responsive cortical stimulation for the treatment of medically intractable partial epilepsy. Neurology 2011;77(13):1295–304.

Morris HH, Lüders H, Lesser RP, Dinner DS, Hahn JF. Transient neuropsychological abnormalities (including Gerstmann's syndrome) during cortical stimulation. Neurology 1984;34:877–83.

Muldoon SF, Costantini J, Webber WRS, Lesser R, Bassett DS. Locally stable brain states predict suppression of epileptic activity by enhanced cognitive effort. NeuroImage Clin 2018;18:599–607.

Nagai Y, Goldstein LH, Fenwick PB, Trimble MR. Clinical efficacy of galvanic skin response biofeedback training in reducing seizures in adult epilepsy: a preliminary randomized controlled study. Epilepsy Behav 2004;5:216–23.

Nacher V, Ledberg A, Deco G, Romo R. Coherent delta-band oscillations between cortical areas correlate with decision making. Proc Natl Acad Sci U S A 2013;110 (37):15085–90.
Najmi AH. Wavelets: A Concise Guide. Baltimore: Johns Hopkins University Press; .
Netoff TI, Clewley R, Arno S, Keck T, White JA. Epilepsy in small-world networks. J Neurosci 2004;24:8075–83.
Noachtar S, Binnie C, Ebersole J, Mauguiere F, Sakamoto A, Westmoreland B. A glossary of terms most commonly used by clinical electroencephalographers and proposal for the report form for the EEG findings. The International Federation of Clinical Neurophysiology. Electroencephalogr Clin Neurophysiol Suppl 1999;52:21–41.
Ojemann GA. Mental arithmetic during human thalamic stimulation. Neuropsychologia 1974;12(1):1–10.
Palva S, Palva JM. Functional roles of alpha-band phase synchronization in local and large-scale cortical networks. Front Psychol 2011;2:204.
Penfield W, Jasper H. Epilepsy and the functional anatomy of the human brain. Boston: Little Brown and Co.; 1954. Pages 713-715, 731-733.
Pfurtscheller G. The cortical activation model (CAM). ProgBrain Res 2006;159:19–27.
Philipose LE, Gottesman RF, Newhart M, Kleinman JT, Herskovits EH, Pawlak MA, et al. Neural regions essential for reading and spelling of words and pseudowords. Ann Neurol 2007;62:481–92.
Pinheiro-Chagas P, Daitch A, Parvizi J, Dehaene S. Brain mechanisms of arithmetic: a crucial role for ventral temporal cortex. J Cog Neurosci 2018;30:1757–72.
Ponten SC, Bartolomei F, Stam CJ. Small-world networks and epilepsy: graph theoretical analysis of intracerebrally recorded mesial temporal lobe seizures. Clin Neurophysiol 2007;118:918–27.
Pouratian N, Cannestra AF, Bookheimer SY, Martin NA, Toga AW. Variability of intraoperative electrocortical stimulation mapping parameters across and within individuals. J Neurosurg 2004;101:458–66.
Quan A, Osorio I, Ohira T, Milton J. Vulnerability to paroxysmal oscillations in delayed neural networks: a basis for nocturnal frontal lobe epilepsy? Chaos 2011;21. 047512–1–9.
Reid N, Crépeau H. Influence functions for proportional hazards regression. Biometrika 1985;72(1):1–9.
Roopun AK, Middleton SJ, Cunningham MO, LeBeau FE, Bibbig A, Whittington MA, et al. A beta2-frequency (20–30 Hz) oscillation in nonsynaptic networks of somatosensory cortex. Proc Natl Acad Sci USA 2006;103(42):15646–50.
Sauseng P, Hoppe J, Klimesch W, Gerloff C, Hummel FC. Dissociation of sustained attention from central executive functions: local activity and interregional connectivity in the theta range. Euro J Neurosci 2007;25:587–93.
Schindler KA, Bialonski S, Horstmann MT, Elger CE, Lehnertz K. Evolving functional network properties and synchronizability during human epileptic seizures. Chaos 2008;18. 033119–1–6.
Shaw JC. Correlation and coherence analysis of the EEG: a selective tutorial review. Int J Psychophysiol 1984;1(3):255–66.
Shenhav A, Musslick S, Lieder F, Kool W, Griffiths TL, Cohen JD, et al. Toward a rational and mechanistic account of mental effort. Ann Rev Neurosci 2017;40:99–124.
Sheybani L, Birot G, Contestabile A, Seeck M, Kiss JZ, Schaller K, et al. Electrophysiological evidence for the development of a self-sustained large-scale epileptic network in the kainate mouse model of temporal lobe epilepsy. J Neurosci 2018;38(15):3776–91.
Siegel M, Donner TH, Engel AK. Spectral fingerprints of large-scale neuronal interactions. Nature Rev Neurosci 2012;13(2):121–34.
Sinai A, Bowers CW, Crainiceanu CM, Boatman D, Gordon B, Lesser RP, et al. Electrocorticographic high gamma activity versus electrical cortical stimulation mapping of naming. Brain 2005;128:1556–70.
Spyropoulos G, Bosman CA, Fries P. A theta rhythm in macaque visual cortex and its attentional modulation. Proc Natl Acad Sci USA 2018;115(24):E5614–23.
Sterman MB, Macdonald LR, Stone RK. Biofeedback training of the sensorimotor electroencephalogram rhythm in man: effects on epilepsy. Epilepsia 1974;15:395–416.
Sterman MB, Shouse MN. Quantitative analysis of training, sleep EEG and clinical response to EEG operant conditioning in epileptics. Electroencephalogr Clin Neurophysiol 1980;49:558–76.
Temkin NR, Davis GR. Stress as a risk factor for seizures among adults with epilepsy. Epilepsia 1984;25:450–6.
Thompson E, Varela FJ. Radical embodiment: neural dynamics and consciousness. Trends Cogn Sci 2001;5:418–25.
Tomlinson SB, Porter BE, Marsh ED. Interictal network synchrony and local heterogeneity predict epilepsy surgery outcome among pediatric patients. Epilepsia 2017;58(3):402–11.
Towle VL, Carder RK, Khorasani L, Lindberg D. Electrocorticographic coherence patterns. J Clin Neurophysiol 1999;16(6):528–47.
Trevelyan AJ, Baldeweg T, van DW, Yuste R, Whittington M. The source of afterdischarge activity in neocortical tonic-clonic epilepsy. J Neurosci 2007;27:13513–9.
Whalen J, McCloskey M, Lesser R, Gordon B. Localizing arithmetic processes in the brain: evidence from a transient deficit during cortical stimulation. J Cogn Neurosci 1997;9:409–17.
Wolf P. The role of nonpharmaceutic conservative interventions in the treatment and secondary prevention of epilepsy. Epilepsia 2002;43(Suppl 9):2–5.
Zarjam P, Epps J, Chen F, Lovell NH. Estimating cognitive workload using wavelet entropy-based features during an arithmetic task. Comput Biol Med 2013;43 (12):2186–95.
Zhang H, Watrous AJ, Patel A, Jacobs J. Theta and alpha oscillations are traveling waves in the human neocortex. Neuron 2018;98(6):1269–81.